Title: Epigenetic repression of Wnt receptors in AD: a role for Sirtuin2-induced H4K16ac deacetylation of Frizzled1 and Frizzled7 promoters

Dr Ernest Palomer[1], Dr Núria Martin-Flores[1], Dr Sarah Jolly[2], Dr Patricia Pascual-Vargas[1], Dr Stefano Benvegnù[2], Dr Marina Podpolny[1], Ms Kadi Vaher[1], Prof Takashi Saito[3], Prof Takaomi C Saido[4], Prof Paul Whiting[2,5], Prof Patricia C Salinas[1*].

[1]Department of Cell and Developmental Biology, University College London, London, United Kingdom.
[2]ARUK-UCL Drug Discovery Institute, University College London, London, United Kingdom.
[3]Laboratory for Cell Signalling, RIKEN Center for Integrative Medical Sciences, Wako-shi, Saitama, Japan.
4Laboratory for Proteolytic Neuroscience, RIKEN Center for Brain Science, Wako-shi, Saitama, Japan.
[5]UK Dementia Research Institute at University College London, London, United Kingdom.
*Corresponding author:
Prof Patricia C Salinas
Department of Cell & Developmental Biology
University College London MRC-LMCB Building, London WC1E 6BT
Tel: +44 (0) 20 7679 2445, email: p.salinas@ucl.ac.uk

KEYWORDS: Alzheimer's Disease, Wnt Signalling, Frizzled Receptors, H4K16ac, Sirt2, PP2C, hAPP$^{NLGF/NLGF}$

ABSTRACT:

Growing evidence supports a role for deficient Wnt signalling in Alzheimer´s disease (AD). First, the Wnt antagonist DKK1 is elevated in the AD brain and is required for amyloid-β-induced synapse loss. Second, LRP6 Wnt co-receptor is required for synapse integrity and three variants of this receptor are linked to late-onset AD. However, the expression/role of other Wnt signalling components remain poorly explored in AD. Wnt receptors Frizzled1 (Fzd1), Fzd5, Fzd7 and Fzd9 are of particular interest due to their role in synapse formation/plasticity. Our analyses showed that *FZD1* and *FZD7* mRNA levels were reduced in the hippocampus of human preclinical AD (PAD) cases and in the $hAPP^{NLGF/NLGF}$ mouse model. This transcriptional downregulation was accompanied by reduced levels of the pro-transcriptional histone mark H4K16ac and a concomitant increase of its deacetylase Sirt2 at *Fzd1* and *Fzd7* promoters in AD. *In vitro* and *in vivo* inhibition of Sirt2 rescued *Fzd1* and *Fzd7* mRNA expression and H4K16ac levels at their promoters. Finally, we found reduced levels of inhibitory phosphorylation on Sirt2 in nuclear PAD samples and increased levels of the Sirt2 phosphatase PP2C, leading to hyperactive nuclear Sirt2 and favouring *Fzd1* and *Fzd7* repression in AD. Collectively, our findings define a novel role for nuclear hyperactivated Sirt2 in repressing *Fzd1* and *Fzd7* expression *via* H4K16ac deacetylation in AD. We propose Sirt2 as an attractive target to ameliorate AD pathology.

Introduction:

Alzheimer's disease (AD) is the most common form of dementia, clinically characterised by progressive cognitive impairment and memory loss. One of the early events in AD is the loss of synapses, a process strongly correlated with cognitive decline (Colom-Cadena et al., 2020; Terry et al., 1991). Interestingly, several signalling pathways required for synapse function and integrity are dysregulated in AD (Forner et al., 2017; Mucke and Selkoe, 2012). Of particular interest is the Wnt signalling pathway(s). First, the secreted Wnt antagonist DKK1 is elevated both in the brain of AD patients and models (Caricasole et al., 2004; Jolly et al., 2019; Rosi et al., 2010) and by exposure to Aβ-oligomers (Purro et al., 2012). Importantly, blockade or knockdown of Dkk1 protects synapses against Aβ (Purro et al., 2012; Sellers et al., 2018). Second, three genetic variants of the Wnt co-receptor Low-Density Lipoprotein Receptor-Related Protein-6 (LRP6) have been linked to late-onset AD (LOAD) (Alarcón et al., 2013; De Ferrari et al., 2007). Third, Wnt3a and Wnt5a are protective against Aβ (Alvarez et al., 2004; Cerpa et al., 2010). Fourth, induced Dkk1 expression in the adult mouse hippocampus leads to synapse loss, plasticity defects and cognitive impairment (Killick et al., 2014; Marzo et al., 2016), features that can be reversed by cessation of Dkk1 expression (Marzo et al., 2016). Together, these findings demonstrate that Aβ deregulates Wnt signalling, a cascade that is crucial for synapse integrity, and that boosting Wnt signalling could be protective in AD.

Deregulation of Wnt signalling in AD could be mediated by different mechanisms; elevation of Wnt antagonists, such as Dkk1, or down-regulation of key Wnt components such as Wnt proteins or their receptor Frizzled (Fzd) (Nusse and Clevers, 2017). Interestingly, several Fzd receptors are sufficient and/or required for synaptic assembly. For example, Fzd1 and Fzd5 are involved in preassembly whereas Fzd7 and Fz9 are involved for the assembly of postsynaptic sites (McLeod et al., 2018; Ramírez et al., 2016; Sahores et al., 2010; Varela-Nallar et al., 2009) (Fig. 1A). Fzd7 is also required for synaptic plasticity (McLeod et al., 2018). However, little is known about how these Fzd receptors are regulated in AD.

Here, we investigated whether Fzd receptors are deregulated in AD and the mechanisms involved. We found that *Fzd1* and *Fzd7* are downregulated in early AD by a shared epigenetic mechanism that depends on the hyperactivity of the nuclear Sirtuin2 (Sirt2). We demonstrated that increased Sirt2 at *Fzd1* and *Fzd7* promoters leads to reduced levels of the active histone mark H4K16ac at their promoters resulting in their transcriptional repression in AD.

RESULTS:

Frizzled1 and *Frizzled7* expression is downregulated in AD

Deficient Wnt signalling has been linked to AD by studies on the Wnt antagonist DKK1 and LRP6 genetic variants (Palomer et al., 2019). However, very little is known about the regulation of Frizzled receptors (Fzd) in AD. Four Fzd receptors (Fzd1, Fzd5, Fzd7 and Fzd9) have been shown to regulate synapse formation and/or function (McLeod et al., 2018; Ramírez et al., 2016; Sahores et al., 2010; Varela-Nallar et al., 2009) (Fig. 1A). We therefore evaluated the expression levels of these receptors at early human AD stages. We performed RT-qPCR on human hippocampal RNA samples from control and subjects with early AD, which have AD histopathological features but no cognitive deficits (preclinical AD; PAD; Supp. Table 1). We found reduced *FZD1* and *FZD7* mRNA levels in PAD samples (Fig. 1B). In contrast, *FZD5* and *FZD9* mRNA levels were unchanged (Fig. 1B). These results suggest that two *Fzd* receptors with synaptic function are downregulated in early stages of AD.

Next, we investigated whether the mRNA levels of these *Fzds* were also affected in an AD model. We used the knock-in AD line hAPP$^{NLGF/NLGF}$ (NLGF), which carries the humanized form of the APP with the Swedish, Iberian and Arctic mutations, leading to Aβ overproduction (Saito et al., 2014). We analysed *Fzd* expression in hippocampal samples of NLGF animals at 2-months-old, a time when Aβ plaques start to appear (Saito et al., 2014). Our results showed reduced levels of *Fzd1* and *Fzd7* expression in NLGF samples, whereas *Fzd5* and *Fzd9* expression remained unchanged (Fig. 1C). Together, these results demonstrate that *Fzd1* and

Fzd7 expression were reduced in both human PAD subjects and the AD mouse model at early disease stages.

Finally, we asked whether reduced mRNA levels of *Fzd1* and *Fzd7* were neuronal specific. We performed single molecule RNA fluorescent in-situ hybridisation (smFISH) for *Fzd1* and *Fzd7* in the CA1 area of the hippocampus (Fig. 1D). Single-cell analyses revealed reduced *Fzd1* levels in NLGF neuronal cells (Rbfox3^{+}), without changes in non-neuronal cells (Rbfox3^{-}; Fig. 1E). However, no overall changes in *Fzd7* levels were observed (Fig. 1F). Next, we analysed the distribution of transcript copy number in neuronal cells. We found that neurons containing ≥3 *Fzd1* transcripts were reduced in AD (Fig. 1G). Interestingly, we observed a reduced number of neurons containing one *Fzd7* transcript in the NLGF (Fig. 1H). The lack of difference in H-score for *Fzd7* could be explained by the lower weighting for percentage of cells with 1 copy (see methods). Altogether, our results demonstrate that *Fzd1* and *Fzd7* RNA levels are reduced in both human PAD and AD mouse model, with a clear downregulation of neuronal *Fzd1* expression and reduced number of neurons containing one *Fzd7* transcript in the AD mouse hippocampus.

Fzd1 and _Fzd7_ promoters present reduced H4K16ac levels with concomitant increase of Sirt2 in AD

The reduced levels of *FZD1* and *FZD7* expression at early AD stages led us to hypothesise that a shared epigenetic regulation could contribute to their dysregulation. A previous study showed that the pro-transcriptional histone mark acetylated Histone H4 Lysine 16 (H4K16ac) is enriched at promoters of several Wnt signalling pathway components (Horikoshi et al., 2013). Chromatin immunoprecipitation (ChIP)-qPCR indeed showed high levels of H4K16ac at *Fzd1* and *Fzd7* promoters, similar to those at *Eif5* (Supp. Fig 1A), a gene reported to have high levels of H4K16ac in the human brain (Nativio et al., 2018). In contrast, *Fzd5* promoter exhibited low levels of H4K16ac (Supp. Fig. 1A), similar to those observed at the repressed gene *Krt16*, which has low levels of H4K16ac (Nativio et al., 2018). These results suggest that H4K16ac is enriched at the *Fzd1* and *Fzd7* promoters and might contribute to their regulation.

Next, we analysed H4K16ac levels in human hippocampal samples from control and PAD. First, we found that H4K16ac levels were not altered by the post-mortem interval (PMI) time in our human hippocampal samples (Supp. Fig. 1B). ChIP-qPCR experiments showed that H4K16ac was reduced at *FZD1* and *FZD7* promoters in PAD (Fig. 2A-B), whereas no changes were observed at the promoters of our internal control *FZD5* (Fig. 2A) or external controls *ACTB* (an active gene) and *HOXA1* (a repressed gene; Supp. Fig. 1C). Changes in H4K16ac levels could arise from nucleosome remodelling or from differential levels of H4K16ac *per se*. We found no changes in nucleosome remodelling when analysed by H4 total levels, thus changes of H4K16ac at *FZD1* and *FZD7* promoters were likely due to reduced H4K16ac levels (Supp. Fig 1D). Next, we analysed H4K16ac levels in the NLGF hippocampus and found reduced acetylation levels only at *Fzd1* and *Fzd7* promoters, without changes in their H4 levels (Fig. 2C, Supp. Fig. 1E-F). Altogether, these results show reduced H4K16ac levels could contribute to *FZD1* and *FZD7* repression in early AD.

Finally, we interrogated which of the three H4K16ac deacetylases (Histone Deacetylases 2 (HDAC), Sirt1 or Sirt2 (Ma and Schultz, 2013; Vaquero et al., 2004, 2006) could be involved in regulating *Fzd1* and *Fzd7* in AD. Interestingly, HDAC2 and Sirt2 play a neurodegenerative role, whereas Sirt1 is neuroprotective (Herskovits and Guarente, 2013; Penney and Tsai, 2014). Therefore, we analysed HDAC2 and Sirt2 occupancy at *Fzds* promoters in early AD. We found no changes HDAC2 levels across all the genes analysed in the hippocampus of NLGF mice (Supp. Fig. 1G). Interestingly, ChIP-qPCR experiments showed an increase in Sirt2 occupancy only at *Fzd1* and *Fzd7* promoters in the hippocampus of AD mice (Fig. 2D, Supp. Fig. 1H). Therefore, our results demonstrate that reduced expression of *Fzd1* and *Fzd7* correlates with reduced levels of H4K16ac and with a concomitant increase of its histone deacetylase Sirt2 at their promoters.

Sirt2 inhibition rescues _Fzds_ epigenome and transcription in AD

To test if Sirt2 deacetylates H4K16ac at *Fzd1* and *Fzd7* promoters in early AD, we prepared hippocampal organotypic cultures (HOC) from WT and NLGF animals. Consistent with our results in PAD and NLGF mice, we found that 15DIV HOC derived from NLGF exhibit reduced H4K16ac levels, increased Sirt2 levels at *Fzd1* and *Fzd7* promoters and a concomitant reduction in their transcription (Supp. Fig. 2A-D). Next, we studied whether Sirt2 regulates *Fzd* transcription using the specific Sirt2 inhibitor AGK2 (Carafa et al., 2016) (Fig. 3A). Cell viability experiments by Fluorescent Activated Cell Sorting (FACS) showed that AGK2 was not toxic (Supp. Fig. 3A, Supp. Table 2) but effectively supressed Sirt2 activity as shown by increased acetylation of the Sirt2 substrate H3K56ac (Bosch-Presegué and Vaquero, 2015) (Supp. Fig. 3B). In addition, RT-qPCR experiments showed that Sirt2 inhibition by AGK2 rescued *Fzd1* and *Fzd7* mRNA expression in the NLGF-HOC, without affecting Fzd5 expression (Fig. 3B-C). To further demonstrate that Sirt2 inhibition rescues *Fzd1* and *Fzd7* mRNA levels, we treated our HOC model with a second specific and structurally distinct Sirt2 inhibitor; AK7 (Supp. Table 2) (Carafa et al., 2016). AK7 treatment was not toxic when analysed by FACS and effectively supressed Sirt2 activity as shown by increased levels of H3K56ac (Fig. 3A, Supp. Fig. 3A, Supp. Fig. 3C). Importantly, Sirt2 inhibition by AK7 rescued *Fzd1* and *Fzd7 mRNA* levels in the NLGF-HOC model, without affecting *Fzd5* mRNAs levels (Fig. 3C-D). Thus, Sirt2 inhibition by two distinct small molecules demonstrate that Sirt2 represses *Fzd1* and *Fzd7* in AD (Fig. 3C). Finally, we analysed whether AK7 treatment also rescued H4K16ac levels in NLGF-HOC. We found that the levels of this pro-transcriptional histone mark were only restored at *Fzd1* and *Fzd7* promoters in the NLGF-HOC treated cultures (Fig. 3E, Supp. Fig. 3D). These results demonstrate that Sirt2 impairs *Fzd1* and *Fzd7* transcription by reducing H4K16ac levels in AD.

To further examine the *in vivo* role of Sirt2 in regulating *Fzd1* and *Fzd7* transcription, we injected the Sirt2 inhibitor AK7 into mice, which crosses the blood brain barrier (Chopra et al., 2012). Mice were injected intraperitoneally with 20 mg/Kg twice a day for 15 days (Fig. 3F), as previously reported (Biella et al., 2016). AK7 administration effectively inhibited Sirt2 in the brain as shown by the increased H3K56ac levels (Supp. Fig. 3E). Sirt2 inhibition rescued *Fzd1* and *Fzd7* expression (Fig. 3G) and H4K16ac levels at their promoters (Fig. 3H) in NLGF animals. Similar to our *in vitro* studies, AK7 did not modulate mRNA or H4K16ac levels of control genes (Fig. 3H, Supp. Fig. 3F). Previous studies using a higher and longer dosage of AK7 linked Sirt2 inhibition with reduced Aβ levels in AD models (Wang et al., 2020). However, we did not find changes in $A\beta_{42}$ levels (Supp. Fig. 3G), as previously reported with the same AK7 dosage in two different AD models (Biella et al., 2016). Collectively, these results show that *Fzd1* and *Fzd7* genes are repressed through Sirt2 deacetylation of H4K16ac in AD (Fig. 3C).

Increased nuclear Sirt2 activity represses *Fzd1* and *Fzd7* in AD

Increased Sirt2 occupancy at *Fzd1* and *Fzd7* promoters suggest that Sirt2 levels might be upregulated in AD. To test this hypothesis, we analysed total SIRT2 protein levels in the hippocampus of PAD human samples and found no changes (Supp. Fig. 4A). Given that Sirt2 is also present in the nucleus (North and Verdin, 2007), we prepared nuclear enriched fractions (Supp. Fig. 4B-C). However, no differences in SIRT2 nuclear levels were observed in PAD samples (Fig. 4A). These results indicate that increased Sirt2 occupancy at *Fzd1* and *Fzd7* promoters does not correlate with increased total/nuclear levels of Sirt2.

Sirt2 activity can be modulated by inhibitory phosphorylation (Pandithage et al., 2008; Pereira et al., 2018). We therefore analysed the phosphorylation state of Sirt2 at its Serine 331 (pSirt2). We found reduced pSIRT2 levels in nuclear fractions of PAD hippocampal samples (Fig. 4A), without changes in total levels (Supp. Fig. 4A). Similarly, lower levels of nuclear pSirt2 were observed in NLGF-HOC model (Supp. Fig. 4D). Decreased levels of Sirt2 inhibitory phosphorylation in early AD could be regulated by specific phosphatases, as the Sirt2 phosphatases PP2Cα (Pereira et al., 2018) is upregulated at the RNA level in an AD mouse model (Gatta et al., 2014). We therefore analysed the expression of the Sirt2 phosphatases PP2Cα/β (Pereira et al., 2018) and found no changes in the total levels of this protein in hippocampal samples from human PAD (Supp. Fig. 4E). Next, we analysed nuclear localisation and found increased levels of PP2Cα, but not PP2Cβ, in PAD subjects (Fig. 4C,

Supp. Fig 4F). Importantly, Pp2cα was also upregulated in nuclear samples of NLGF-HOC (Supp. Fig. 4G). These results suggest that increased nuclear levels of PP2C could lead to Sirt2 hyperactivity in the nucleus, thus favouring the repression of *Fzd1* and *Fzd7* in AD.

To establish the role of PP2C in *Fzd1* and *Fzd7* expression in AD, HOC were treated with a non-toxic concentration of sanguinarine (SAN), a PP2C specific inhibitor (Kimura et al., 2010) (Fig. 4B, Supp. Fig 4H, Supp. Table. 2). Next, we analysed the impact of SAN on the expression of *Fzd1* and *Fzd7*. Our results showed that Pp2c inhibition rescued *Fzd1* and *Fzd7* expression and H4K16ac levels in the NLGF-HOCs, without affecting the control genes (Fig. 4D-E, Supp. Fig. 4I). We found increased pSirt2 only in NLGF-HOC SAN-treated samples (Supp. Fig. 4J), supporting the idea that increased nuclear Pp2c levels are responsible for hyperactive Sirt2, leading to *Fzd1* and *Fzd7* repression in AD. Altogether these results demonstrate that Pp2c is upstream of Sirt2 in regulating *Fzd1* and *Fzd7* expression in early AD (Fig. 4F).

DISCUSSION:

In this study, we present novel findings demonstrating that synaptic Wnt signalling receptors *Fzd1* and *Fzd7* are epigenetically downregulated in AD by Sirt2. We found that the phosphatase Pp2cα dephosphorylates nuclear Sirt2, activating this histone deacetylase in AD. In addition, we show that increased Sirt2 levels and a concomitant H4K16ac deacetylation at *Fzd1* and *Fzd7* promoters favours *Fzd1* and *Fzd7* transcriptional repression in AD (Fig. 5).

Wnt signalling has been linked to AD by the identification of three LRP6 genetic variants and by a large body of research demonstrating the synaptotoxic role of the Wnt antagonist Dkk1 in AD (Alarcón et al., 2013; De Ferrari et al., 2007; Purro et al., 2012; Sellers et al., 2018). Here, we report for the first time that two Fzds with synaptic function display reduced expression in the hippocampus of PAD patients and 2-month-old NLGF model. Our results showed a reduction in neuronal *Fzd1* and *Fzd7* expression in AD. Interestingly, Fzd1 and Fzd7 are localised at the pre- and post-synaptic side respectively (McLeod et al., 2018; Varela-Nallar et al., 2009), thus their reduced levels could impact both sides of the synapse. Postsynaptically, Fzd7 is required for spine formation and LTP *in vitro* (McLeod et al., 2018) and for dendritic arborization during postnatal development *in vivo* (Ferrari et al., 2018). At the presynaptic site, Fzd1 is sufficient and required for presynaptic assembly(Varela-Nallar et al., 2009). Interestingly, Wnt3a prevents Aβ-induced synapse loss in a Fzd1-dependent manner (Chacón et al., 2008). We observe reduced Fzd1 expression, which could contribute to synapse vulnerability in AD. Together, these results suggest that reduced levels of Fzd1 and Fzd7 could contribute to the impaired synaptic plasticity and synapse loss observed in early AD.

Fzd1 and *Fzd7* expression are regulated by epigenetic mechanisms such as noncoding RNAs and DNA methylation in different biological processes and diseases (Li et al., 2011; Salpea et al., 2012; Wu et al., 2019; Zhang et al., 2011). In this study, we demonstrated a novel role for Sirt2 in repressing *Fzd1* and *Fzd7* by deacetylating H4K16ac at their promoters in AD (Fig. 5). Sirt2 has other histone substrates, including H3K18ac and H3K56ac (Bosch-Presegué and Vaquero, 2015). However, we found no differences in these histone marks (Supp. Fig. 5A-B), suggesting a specific H4K16 deacetylation by Sirt2 at *Fzd1* and *Fzd7* promoters in AD. Interestingly, H4K16ac has been linked to Fzds regulation in brain development: H4K16ac deacetylation by Sirt1 regulates *Fzd5* and *Fzd7* transcription during cortical neurogenesis (Bonnefont et al., 2019). Together with our results, this data strongly suggest that H4K16ac deacetylation regulates the transcription of different *Fzds* in development and neurodegeneration These studies also show different roles for Sirt1 and Sirt2, consistent with the idea that Sirt1 is neuroprotective whereas Sirt2 plays a neurodegenerative role (Herskovits and Guarente, 2013; Penney and Tsai, 2014).

Increasing evidence suggests a neurodegenerative role for Sirt2. First, a genetic variant of *SIRT2* is linked to LOAD in *APOEε4*-negative population (Cacabelos et al., 2019). Second, *in vivo* Sirt2 inhibition improves cognition in three AD models (Biella et al., 2016; Wang et al., 2020). Third, increased SIRT2 levels are observed in a cellular AD model (Esteves et al., 2019;

Silva et al., 2017). However, our results show no changes in SIRT2 levels in human hippocampal PAD samples. Interestingly, we observed a specific reduction of Sirt2 phosphorylation in nuclear fractions of PAD patients, a post-translational modification known to inhibit Sirt2 deacetylase activity (Pandithage et al., 2008; Pereira et al., 2018). These results suggest the presence of hyperactive nuclear Sirt2 in AD. We also showed increased nuclear levels of PP2Cα, a Sirt2 phosphatase, in PAD subjects, in line with previous results showing increased mRNA levels of PP2Cα in an AD mouse model (Gatta et al., 2014). Consistently, we found that PP2C-induced nuclear Sirt2 hyperactivity is upstream of H4K16 deacetylation by Sirt2 at *Fzd1* and *Fzd7* promoter in AD (Fig. 5), demonstrating for the first time a role for PP2C in AD. Taken together, our results demonstrate a new role for nuclear hyperactive Sirt2, leading to *Fzd1* and *Fzd7* epigenetic repression. This mechanism could also regulate other genes implicated in AD. Moreover, the epigenetic regulation of Wnt receptors by the Sirt2-H4K16ac could also modulate these genes in other cellular contexts.

In summary, we report a novel role for nuclear Sirt2 in regulating *Fzd* receptors in AD. We propose that nuclear Sirt2 is hyperactivated in AD and recruited to *Fzd1* and *Fzd7* promoters leading to reduced H4K16ac, which in turn impairs their transcription. Thus, Sirt2 is a promising target for developing new AD therapies to restore the expression of key Wnt receptors.

EXPERIMENTAL PROCEDURES:

Human Tissue

Anonymised human hippocampal samples from control and presymptomatic AD subjects were obtained from Cambridge Brain Bank, Division of the Human Research Tissue Bank, Addenbrooke's Hospital, Cambridge UK. All samples were obtained with informed consent under CBB license (NRES 10/HO308/56). Tissues were stored at -80°C. Demographic data and Braak stages for each sample set are shown in Supp. Table 1.

Animals

All procedures involving animals were conducted according to the Animals Scientific Procedures Act UK (1986) and in compliance with the ethical standards at University College London (UCL). $APP^{NLGF/NLGF}$ knock-in and WT littermates were used in this study. Genotyping was performed using DNA from ear biopsies as previously described (Saito et al., 2014). Animals were kept in ventilated racks at 22±2°C and 55±10% humidity with a 12h/12h light cycle and free access to food and water at all times.

Statistical analysis

All values are presented as mean + SEM. Statistical analyses were performed using SPSS v25 (IBM). Outliers were determined with the explore tool, based on multiplying the Interquartile Range by a factor of 1.5. Data normality and homogeneity of variances were tested by the Shapiro-Wilk and Levene tests, respectively. Mann-Whitney U-test (two groups) or Kruskal-Wallis followed by Dunn's multiple comparison (more than two groups) tests were used for non-normally distributed datasets. For normally distributed data; Student's t-test (two groups) or two-way ANOVA (more than two groups) followed by post hoc pair-wise comparisons assuming (Tukey's) or not assuming equal variances (Games-Howell). In the figures, asterisks indicate p values as follows: $^{*}p < 0.05$; $^{**}p < 0.01$; $^{***}p < 0.001$.

SUPPLEMENTARY INFORMATION:

For further information see Supplementary Figures, Supplementary Methods and Supplementary Tables.

AUTHOR'S CONTRIBUTION:

E.P. and P.C.S. conceived this study. E.P., N.MF, M.P. and K.V. performed *in vivo* experiments. E.P., S.J. and P.W. performed smFISH and experiments in human samples. E.P., P.P-V. and S.B. performed *in vitro* experiments. T.S. and T.C.S. provided the $hAPP^{NLGF/NLGF}$ line. E.P. and P.C.S. wrote the manuscript with input from all authors.

ACKNOWLEDGMENTS/FUNDINGS:
This work was funded by the MRC (P.C.S.: MR/M024083/1), Alzheimer's Society (P.C.S.: AS-PG-18-008), Alzheimer's Research UK (P.C.S. and E.P.: ARUK-PG2018A-002; P.W.: ARUK-2018DDI-UCL), European Commission Horizon 2020 (E.P.: H2020 MSCA-IF 749209).

CONFLICTS OF INTEREST:
None.

FIGURE LEGENES:

Figure 1: *Frizzled1* and *Frizzled7* expression is downregulated in early AD
A) Schematic showing the localization of Fzd1, Fzd5, Fzd7 and Fzd9 at the pre- and/or post-synaptic sides and the action of Wnts on both sites of the synapse. B) qPCR analyses showed reduced mRNA levels of *FZD1* and *FZD7* in human hippocampal samples from preclinical AD (PAD) subjects compared to controls (CNT). No changes were observed in the levels of *FZD5* and *FZD9* mRNAs at early AD. C) qPCR analyses showed reduced mRNA levels of *Fzd1* and *Fzd7* in 2-month-old NLGF hippocampus. No differences in *Fzd5* and *Fzd9* levels were observed in NLGF mice. D) Representative smFISH images of WT and NLGF CA1 hippocampal region. Top row shows merged images with DAPI (blue), *Fzd1* (green), *Fzd7* (yellow) and *Rbfox3* (magenta) mRNAs. *Fzd1* in black (second row) and its representative neuronal *Rbfox3*$^+$ cells corresponding to 3 and >3 *Fzd1* copies (third row). *Fzd7* in black (fourth row) and its representative cells corresponding to one *Fzd7* copy (fifth row). Scale bars represent 50 µm and 12.5 µm in the zoomed in inserts. E-F) Single-cell analyses expressed as H-score for *Fzd1* (E) and *Fzd7* (F) in neuronal (*Rbfox3*$^+$) and non-neuronal (*Rbfoz3*$^-$) cells. G-H) Single-cell distribution of neurons (*Rbfox3*$^+$) containing 1, 2, 3 or >3 transcripts for *Fzd1* (G) or *Fzd7* (H). Data are represented as mean + SEM. Statistical analysis by *t*-test in B for *FZD1*, *FZD7* and *FZD9* and by Mann-Whitney for *FZD5*; in C *t*-test for all genes analysed; in E and F *t*-test for neuronal and non-neuronal; in G *t*-test for 1, 2 and 3 copies and by Mann-Whitney for >3 copies; in H *t*-test for 1 and 2 copies and by Mann-Whitney for 3 and >3 copies. Values inside bars indicate number of samples; asterisks indicate *$p<0.05$; **$p<0.01$.

Figure 2: Downregulation of *Fzds* in AD correlates with reduced levels of H4K16ac and the concomitant increase in Sirt2 at *Fzds* promoters
A) ChIP-qPCR analyses showed reduced H4K16ac levels at *FZD1* and *FZD7* promoters in preclinical AD subjects (PAD). H4K16ac levels remained unchanged at *FZD5* promoter. B) Scheme representing the epigenetic changes observed in AD, where *Fzd1* and *Fzd7* promoters present reduced levels of H4K16ac and increased levels of the histone deacetylase Sirt2. C) ChIP-qPCR experiments showed reduced H4K16ac at *Fzd1* and *Fzd7* promoters in NLGF hippocampal samples. No changes were observed for *Fzd5*. D) ChIP-qPCR analyses demonstrated increased levels of Sirt2 at the promoters of *Fzd1* and *Fzd7* in NLGF hippocampal samples when compared to controls. No differences were observed at *Fzd5* promoter. Data are represented as mean + SEM. Statistical analyses by *t*-test in A for *FZD1*, *FZD7* and by Mann-Whitney for *FZD5*; in C *t-t*est for *Fzd1* and *Fzd5* and by Mann-Whitney for *Fzd7*; in D *t*-test for *Fzd1*, *Fzd7*, *Fzd5*. Values inside bars indicate number of samples; asterisks indicate *$p<0.05$; **$p<0.01$.

Figure 3: Sirt2 inhibition rescues *Fzds* epigenome and transcription in AD
A) Scheme representing AGK2 and AK7 treatments of HOC. Hippocampal slices were cultured for 15 DIV and treated with 7 µM of AGK2 for 72 hours or with 30 µM of AK7 for 7 days. B) qPCR analyses of mRNA levels from WT and NLGF hippocampal cultures treated with vehicle or AGK2. Our results showed that AGK2 treatment rescues *Fzd1* and *Fzd7* mRNA levels without modulating *Fzd5* mRNA levels. C) Scheme representing the epigenetic state of *Fzd1* and *Fzd7* promoters in AD and how Sirt2 inhibition rescues H4K16ac levels and their mRNA expression. D) qPCR results show that Sirt2 inhibition by AK7 rescued *Fzd1* and *Fzd7* mRNA levels in AD treated cultures, without modulating *Fzd5* mRNA levels. E) ChIP-qPCR showing that AK7 treatment rescued the levels of H4K16ac at *Fzd1* and *Fzd7* promoters in NLGF-HOC while not changing the levels of H4K16ac in WT or at *Fz5* promoter. F) Scheme showing the dosage regime for *in vivo* inhibition of Sirt2 by intraperitoneal injections of 20 mg/Kg of AK7

twice a day for 15 days, from 1.5 to 2-months-old WT and NLGF animals. G) qPCR analyses of mRNA levels from WT and NLGF hippocampal samples treated with vehicle or AK7. Our results showed that AK7 rescued *Fzd1* and *Fzd7* mRNA levels back to WT in NLGF treated animals and did not show any effect on *Fzd5* mRNA levels. H) ChIP-qPCR showed that Sirt2 inhibition by AK7 rescued the levels of H4K16ac at *Fzd1* and *Fzd7* promoters in AD while no changes were observed in WT or at *Fzd5* promoter. Data are represented as mean + SEM. Statistical analyses by Two-way ANOVA followed by Tukey's post hoc in B for all genes analysed; in D Two-way ANOVA followed by Tukey's post hoc for *Fzd1* and *Fzd7* and Kruskal-Wallis followed by Dunn's multiple comparison for *Fzd5*; in E Kruskal-Wallis followed by Dunn's multiple comparison for all genes analysed; in G Two-way ANOVA followed by Tukey's post hoc for *Fzd1* and *Fzd7* and Kruskal-Wallis followed by Dunn's multiple comparison for *Fzd5*; in H Two-way ANOVA followed by Tukey's post hoc for *Fzd1* and *Fzd5* and Two-way ANOVA followed by Games-Howell post hoc for *Fzd7*. Values inside bars indicate number of samples; asterisks indicate *p<0.05; **p<0.01; ***p<0.005.

Figure 4: Increased Sirt2 activity in AD impairs *Fzds* transcription
A) WB analyses of total and pSirt2 levels in hippocampal nuclear extracts of human control/PAD subjects showing decreased levels of pSirt2.2 at early AD. B) Scheme representing Sanguinarine (SAN) treatment in the *in vitro* AD organotypic model for 7 days. C) WB analyses of PP2Cα in hippocampal nuclear extracts of human control/PAD subjects, sowing increased levels of PP2Cα in human PAD group. D) qPCR analyses of total mRNA levels from WT and $hAPP^{NLGF/NLGF}$ hippocampal samples treated with vehicle or SAN. Our results show that SAN treatment rescues *Fzd1* and *Fzd7* mRNA levels and does not show any effect on *Fzd5* mRNA levels. E) ChIP-qPCR showing that SAN treatment rescues the levels of H4K16ac at *Fzd1* and *Fzd7* promoters in AD while not changing are observed in WT or at *Fzd5* promoter. F) Scheme representing increased nuclear levels of the phosphatase PP2C in AD and how PP2C inhibition in AD rescues H4K16ac levels at Fzd1 and Fzd7 promoters and their transcription. Data are represented as mean + SEM. Statistical analyses by *t*-Test in A for total Sirt2.2 and nuclear Sirt2.1 and Srit2.2, and by Mann-Whitney for total Sirt2.1; in D by *t*-Test; in F Two-way ANOVA followed by Tukey's post hoc for *Fzd1* and *Fzd7* and Kruskal-Wallis followed by Dunn's multiple comparison for *Fzd5*; in E Two-way ANOVA followed by Tukey's post hoc for *Fzd7* and Kruskal-Wallis followed by Dunn's multiple comparison for *Fzd1* and *Fzd5*. The value inside bars indicates number of samples; asterisks indicate *p<0.05; **p<0.01; ***p<0.005.

Figure 5: Schematic model of Fzd1 and Fzd7 regulation by Sirt2 in AD
Scheme representing the nuclear localization of the histone deacetylase Sirt2, its phosphatase PP2C and the epigenetic regulation of *Fzd1* and *Fzd7* in healthy and in the early AD brain. In the healthy brain, high levels of H4K16ac and low levels of Sirt2 coexist at *Fzd1* and *Fzd7* promoters, leading to *Fzd1* and *Fzd7* transcription. At early AD stages, increased nuclear levels of the phosphatase PP2C activates Sirt2 by removing its inhibitory phosphorylation. In addition, increased Sirt2 recruitment to *Fzd1* and *Fzd7* promoters leads to reduced levels of H4K16ac and impairing *Fzd1* and *Fzd7* transcription.

REFERENCES:
Alarcón, M.A., Medina, M.A., Hu, Q., Avila, M.E., Bustos, B.I., Pérez-Palma, E., Peralta, A., Salazar, P., Ugarte, G.D., Reyes, A.E., et al. (2013). A novel functional low-density lipoprotein receptor-related protein 6 gene alternative splice variant is associated with Alzheimer's disease. Neurobiol. Aging *34*, 1709.e9-18.
Alvarez, A.R., Godoy, J.A., Mullendorff, K., Olivares, G.H., Bronfman, M., and Inestrosa, N.C. (2004). Wnt-3a overcomes beta-amyloid toxicity in rat hippocampal neurons. Exp. Cell Res. *297*, 186–196.
Biella, G., Fusco, F., Nardo, E., Bernocchi, O., Colombo, A., Lichtenthaler, S.F., Forloni, G., and Albani, D. (2016). Sirtuin 2 Inhibition Improves Cognitive Performance and Acts on Amyloid-β Protein Precursor Processing in Two Alzheimer's Disease Mouse Models. J. Alzheimers. Dis. *53*, 1193–1207.

Bonnefont, J., Tiberi, L., Van Den Ameele, J., Potier, D., Gaber, Z.B., Lin, X., Line Bilheu, A., Le Herpoel, A., Velez Bravo, F.D., Ois Guillemot, F., et al. (2019). Cortical Neurogenesis Requires Bcl6-Mediated Transcriptional Repression of Multiple Self-Renewal-Promoting Extrinsic Pathways Article Cortical Neurogenesis Requires Bcl6-Mediated Transcriptional Repression of Multiple Self-Renewal-Promoting Extrinsic Pathways. Neuron *103*, 1096-1108.e4.
Bosch-Presegué, L., and Vaquero, A. (2015). Sirtuin-dependent epigenetic regulation in the maintenance of genome integrity. FEBS J. *282*, 1745–1767.
Cacabelos, R., Carril, J.C., Cacabelos, N., Kazantsev, A.G., Vostrov, A. V., Corzo, L., Cacabelos, P., and Goldgaber, D. (2019). Sirtuins in alzheimer's disease: SIRT2-related genophenotypes and implications for pharmacoepigenetics. Int. J. Mol. Sci. *20*.
Carafa, V., Rotili, D., Forgione, M., Cuomo, F., Serretiello, E., Hailu, G.S., Jarho, E., Lahtela-Kakkonen, M., Mai, A., and Altucci, L. (2016). Sirtuin functions and modulation: from chemistry to the clinic. Clin. Epigenetics *8*.
Caricasole, A., Copani, A., Caraci, F., Aronica, E., Rozemuller, A.J., Caruso, A., Storto, M., Gaviraghi, G., Terstappen, G.C., and Nicoletti, F. (2004). Induction of Dickkopf-1, a Negative Modulator of the Wnt Pathway, Is Associated with Neuronal Degeneration in Alzheimer's Brain. J. Neurosci. *24*, 6021–6027.
Cerpa, W., Farías, G.G., Godoy, J.A., Fuenzalida, M., Bonansco, C., and Inestrosa, N.C. (2010). Wnt-5a occludes Abeta oligomer-induced depression of glutamatergic transmission in hippocampal neurons. Mol. Neurodegener. *5*, 3.
Chacón, M.A., Varela-Nallar, L., and Inestrosa, N.C. (2008). Frizzled-1 is involved in the neuroprotective effect of Wnt3a against Abeta oligomers. J. Cell. Physiol. *217*, 215–227.
Chopra, V., Quinti, L., Kim, J., Vollor, L., Narayanan, K.L., Edgerly, C., Cipicchio, P.M., Lauver, M.A., Choi, S.H., Silverman, R.B., et al. (2012). The Sirtuin 2 Inhibitor AK-7 Is Neuroprotective in Huntington's Disease Mouse Models. Cell Rep. *2*, 1492–1497.
Colom-Cadena, M., Spires-Jones, T., Zetterberg, H., Blennow, K., Caggiano, A., DeKosky, S.T., Fillit, H., Harrison, J.E., Schneider, L.S., Scheltens, P., et al. (2020). The clinical promise of biomarkers of synapse damage or loss in Alzheimer's disease. Alzheimers. Res. Ther. *12*, 21.
Esteves, A.R., Palma, A.M., Gomes, R., Santos, D., Silva, D.F., and Cardoso, S.M. (2019). Acetylation as a major determinant to microtubule-dependent autophagy: Relevance to Alzheimer's and Parkinson disease pathology. Biochim. Biophys. Acta - Mol. Basis Dis. *1865*, 2008–2023.
Ferrari, M.E., Bernis, M.E., McLeod, F., Podpolny, M., Coullery, R.P., Casadei, I.M., Salinas, P.C., and Rosso, S.B. (2018). Wnt7b signalling through Frizzled-7 receptor promotes dendrite development by coactivating CaMKII and JNK. J. Cell Sci. *131*.
De Ferrari, G. V, Papassotiropoulos, A., Biechele, T., Wavrant De-Vrieze, F., Avila, M.E., Major, M.B., Myers, A., Sáez, K., Henríquez, J.P., Zhao, A., et al. (2007). Common genetic variation within the low-density lipoprotein receptor-related protein 6 and late-onset Alzheimer's disease. Proc. Natl. Acad. Sci. U. S. A. *104*, 9434–9439.
Forner, S., Baglietto-Vargas, D., Martini, A.C., Trujillo-Estrada, L., and LaFerla, F.M. (2017). Synaptic Impairment in Alzheimer's Disease: A Dysregulated Symphony. Trends Neurosci. *40*, 347–357.
Gatta, V., D'Aurora, M., Granzotto, A., Stuppia, L., and Sensi, S.L. (2014). Early and sustained altered expression of aging-related genes in young 3xTg-AD mice. Cell Death Dis. *5*, e1054.
Herskovits, A.Z., and Guarente, L. (2013). Sirtuin deacetylases in neurodegenerative diseases of aging. Cell Res. *23*, 746–758.
Horikoshi, N., Kumar, P., Sharma, G.G., Chen, M., Hunt, C.R., Westover, K., Chowdhury, S., and Pandita, T.K. (2013). Genome-wide distribution of histone H4 Lysine 16 acetylation sites and their relationship to gene expression. Genome Integr. *4*, 3.
Jolly, S., Lang, V., Koelzer, V.H., Sala Frigerio, C., Magno, L., Salinas, P.C., Whiting, P., and Palomer, E. (2019). Single-Cell Quantification of mRNA Expression in The Human Brain. Sci. RepoRtS | *9*, 12353.
Killick, R., Ribe, E.M., Al-Shawi, R., Malik, B., Hooper, C., Fernandes, C., Dobson, R., Nolan, P.M., Lourdusamy, A., Furney, S., et al. (2014). Clusterin regulates β-amyloid toxicity via Dickkopf-1-driven induction of the wnt-PCP-JNK pathway. Mol. Psychiatry *19*, 88–98.

Kimura, K.I., Aburai, N., Yoshida, M., and Ohnishi, M. (2010). Sanguinarine as a potent and specific inhibitor of protein phosphatase 2C in vitro and induces apoptosis via phosphorylation of p38 in HL60 cells. Biosci. Biotechnol. Biochem. *74*, 548–552.
Li, G., Luna, C., Qiu, J., Epstein, D.L., and Gonzalez, P. (2011). Role of miR-204 in the regulation of apoptosis, endoplasmic reticulum stress response, and inflammation in human trabecular meshwork cells. Investig. Ophthalmol. Vis. Sci. *52*, 2999–3007.
Ma, P., and Schultz, R.M. (2013). Histone Deacetylase 2 (HDAC2) Regulates Chromosome Segregation and Kinetochore Function via H4K16 Deacetylation during Oocyte Maturation in Mouse. PLoS Genet. *9*.
Marzo, A., Galli, S., Lopes, D., McLeod, F., Podpolny, M., Segovia-Roldan, M., Ciani, L., Purro, S., Cacucci, F., Gibb, A., et al. (2016). Reversal of synapse degeneration by restoring Wnt signalling in the adult hippocampus. Curr. Biol. *26*, 2551–2561.
McLeod, F., Bossio, A., Marzo, A., Ciani, L., Sibilla, S., Hannan, S., Wilson, G.A., Palomer, E., Smart, T.G., Gibb, A., et al. (2018). Wnt Signaling Mediates LTP-Dependent Spine Plasticity and AMPAR Localization through Frizzled-7 Receptors. Cell Rep. *23*, 1060–1071.
Mucke, L., and Selkoe, D.J. (2012). Neurotoxicity of amyloid β-protein: synaptic and network dysfunction. Cold Spring Harb. Perspect. Med. *2*, a006338.
Nativio, R., Donahue, G., Berson, A., Lan, Y., Amlie-Wolf, A., Tuzer, F., Toledo, J.B., Gosai, S.J., Gregory, B.D., Torres, C., et al. (2018). Dysregulation of the epigenetic landscape of normal aging in Alzheimer's disease. Nat. Neurosci. *21*, 497–505.
North, B.J., and Verdin, E. (2007). Mitotic regulation of SIRT2 by cyclin-dependent kinase 1-dependent phosphorylation. J. Biol. Chem. *282*, 19546–19555.
Nusse, R., and Clevers, H. (2017). Wnt/β-Catenin Signaling, Disease, and Emerging Therapeutic Modalities. Cell *169*, 985–999.
Palomer, E., Buechler, J., and Salinas, P.C. (2019). Wnt signaling deregulation in the aging and Alzheimer's brain. Front. Cell. Neurosci. *13*.
Pandithage, R., Lilischkis, R., Harting, K., Wolf, A., Jedamzik, B., Lüscher-Firzlaff, J., Vervoorts, J., Lasonder, E., Kremmer, E., Knöll, B., et al. (2008). The regulation of SIRT2 function by cyclin-dependent kinases affects cell motility. J. Cell Biol. *180*, 915–929.
Penney, J., and Tsai, L.H. (2014). Histone deacetylases in memory and cognition. Sci. Signal. *7*, re12–re12.
Pereira, J.M., Chevalier, C., Chaze, T., Gianetto, Q., Impens, F., Matondo, M., Cossart, P., and Hamon, M.A. (2018). Infection Reveals a Modification of SIRT2 Critical for Chromatin Association. Cell Rep. *23*, 1124–1137.
Purro, S.A., Dickins, E.M., and Salinas, P.C. (2012). The Secreted Wnt Antagonist Dickkopf-1 Is Required for Amyloid -Mediated Synaptic Loss. J. Neurosci. *32*, 3492–3498.
Ramírez, V.T., Ramos-Fernández, E., Henríquez, J.P., Lorenzo, A., and Inestrosa, N.C. (2016). Wnt-5a/frizzled9 receptor signaling through the Gαo-Gβγ complex regulates dendritic spine formation. J. Biol. Chem. *291*, 19092–19107.
Rosi, M.C., Luccarini, I., Grossi, C., Fiorentini, A., Spillantini, M.G., Prisco, A., Scali, C., Gianfriddo, M., Caricasole, A., Terstappen, G.C., et al. (2010). Increased Dickkopf-1 expression in transgenic mouse models of neurodegenerative disease. *112*, 1539–1551.
Sahores, M., Gibb, A., and Salinas, P.C. (2010). Frizzled-5, a receptor for the synaptic organizer Wnt7a, regulates activity-mediated synaptogenesis. Development *137*, 2215–2225.
Saito, T., Matsuba, Y., Mihira, N., Takano, J., Nilsson, P., Itohara, S., Iwata, N., and Saido, T.C. (2014). Single App knock-in mouse models of Alzheimer's disease. Nat. Neurosci. *17*, 661–663.
Salpea, P., Russanova, V.R., Hirai, T.H., Sourlingas, T.G., Sekeri-Pataryas, K.E., Romero, R., Epstein, J., and Howard, B.H. (2012). Postnatal development-and age-related changes in DNA-methylation patterns in the human genome. Nucleic Acids Res. *40*, 6477–6494.
Sellers, K.J., Elliott, C., Jackson, J., Ghosh, A., Ribe, E., Rojo, A.I., Jarosz-Griffiths, H.H., Watson, I.A., Xia, W., Semenov, M., et al. (2018). Amyloid β synaptotoxicity is Wnt-PCP dependent and blocked by fasudil. Alzheimers. Dement. *14*, 306–317.
Silva, D.F., Esteves, A.R., Oliveira, C.R., and Cardoso, S.M. (2017). Mitochondrial Metabolism Power SIRT2-Dependent Deficient Traffic Causing Alzheimer's-Disease Related Pathology. Mol. Neurobiol. *54*, 4021–4040.
Terry, R.D., Masliah, E., Salmon, D.P., Butters, N., DeTeresa, R., Hill, R., Hansen, L.A., and

Katzman, R. (1991). Physical basis of cognitive alterations in alzheimer's disease: Synapse loss is the major correlate of cognitive impairment. Ann. Neurol. *30*, 572–580.
Vaquero, A., Scher, M., Lee, D., Erdjument-Bromage, H., Tempst, P., and Reinberg, D. (2004). Human SirT1 interacts with histone H1 and promotes formation of facultative heterochromatin. Mol. Cell *16*, 93–105.
Vaquero, A., Scher, M.B., Dong, H.L., Sutton, A., Cheng, H.L., Alt, F.W., Serrano, L., Sternglanz, R., and Reinberg, D. (2006). SirT2 is a histone deacetylase with preference for histone H4 Lys 16 during mitosis. Genes Dev. *20*, 1256–1261.
Varela-Nallar, L., Grabowski, C.P., Alfaro, I.E., Alvarez, A.R., and Inestrosa, N.C. (2009). Role of the Wnt receptor Frizzled-1 in presynaptic differentiation and function. Neural Dev. *4*, 41.
Wang, Y., Yang, J., Hong, T.-T., Sun, Y., Huang, H., Chen, F., Chen, X., Chen, H., Dong, S., Cui, L., et al. (2020). RTN4B-mediated suppression of Sirtuin 2 activity ameliorates β-amyloid pathology and cognitive impairment in Alzheimer's disease mouse model. Aging Cell *19*.
Wu, F., Jiao, J., Liu, F., Yang, Y., Zhang, S., Fang, Z., Dai, Z., and Sun, Z. (2019). Hypermethylation of Frizzled1 is associated with Wnt/β-catenin signaling inactivation in mesenchymal stem cells of patients with steroid-associated osteonecrosis. Exp. Mol. Med. *51*, 1–9.
Zhang, H., Hao, Y., Yang, J., Zhou, Y., Li, J., Yin, S., Sun, C., Ma, M., Huang, Y., and Xi, J.J. (2011). Genome-wide functional screening of miR-23b as a pleiotropic modulator suppressing cancer metastasis. Nat. Commun. *2*, 1–11.

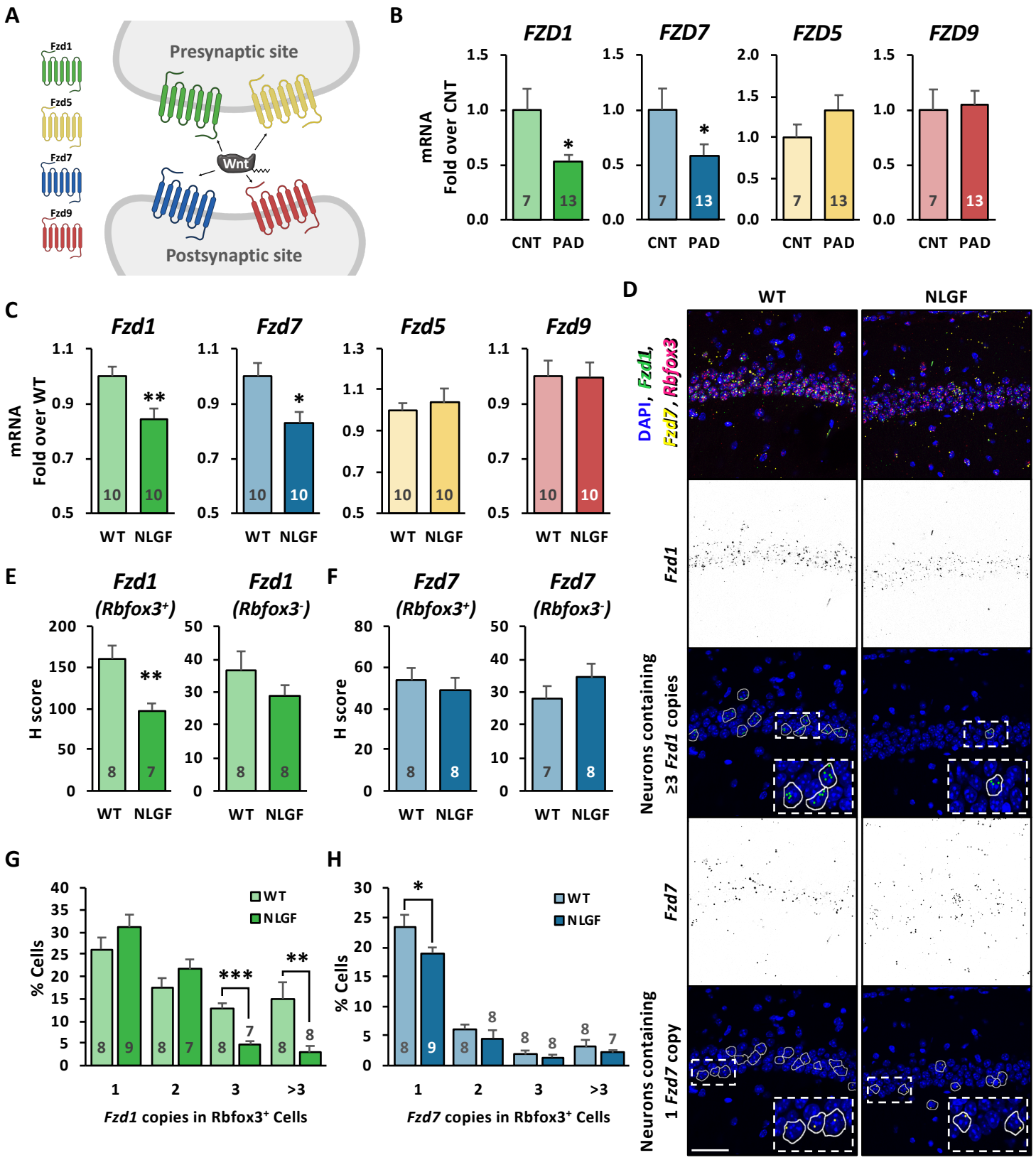
A
Fzd1
Fzd5
Fzd7
Fzd9
Presynaptic site
Wnt
Postsynaptic site
B
FZD1
FZD7
FZD5
FZD9
mRNA
Fold over CNT
CNT PAD
C
Fzd1
Fzd7
Fzd5
Fzd9
mRNA
Fold over WT
WT NLGF
D
WT
NLGF
DAPI, Fzd1, Fzd7, Rbfox3
Fzd1
Neurons containing ≥3 Fzd1 copies
Fzd7
Neurons containing 1 Fzd7 copy
E
Fzd1 (Rbfox3+)
Fzd1 (Rbfox3-)
H score
F
Fzd7 (Rbfox3+)
Fzd7 (Rbfox3-)
G
% Cells
Fzd1 copies in Rbfox3+ Cells
H
Fzd7 copies in Rbfox3+ Cells

Figure1

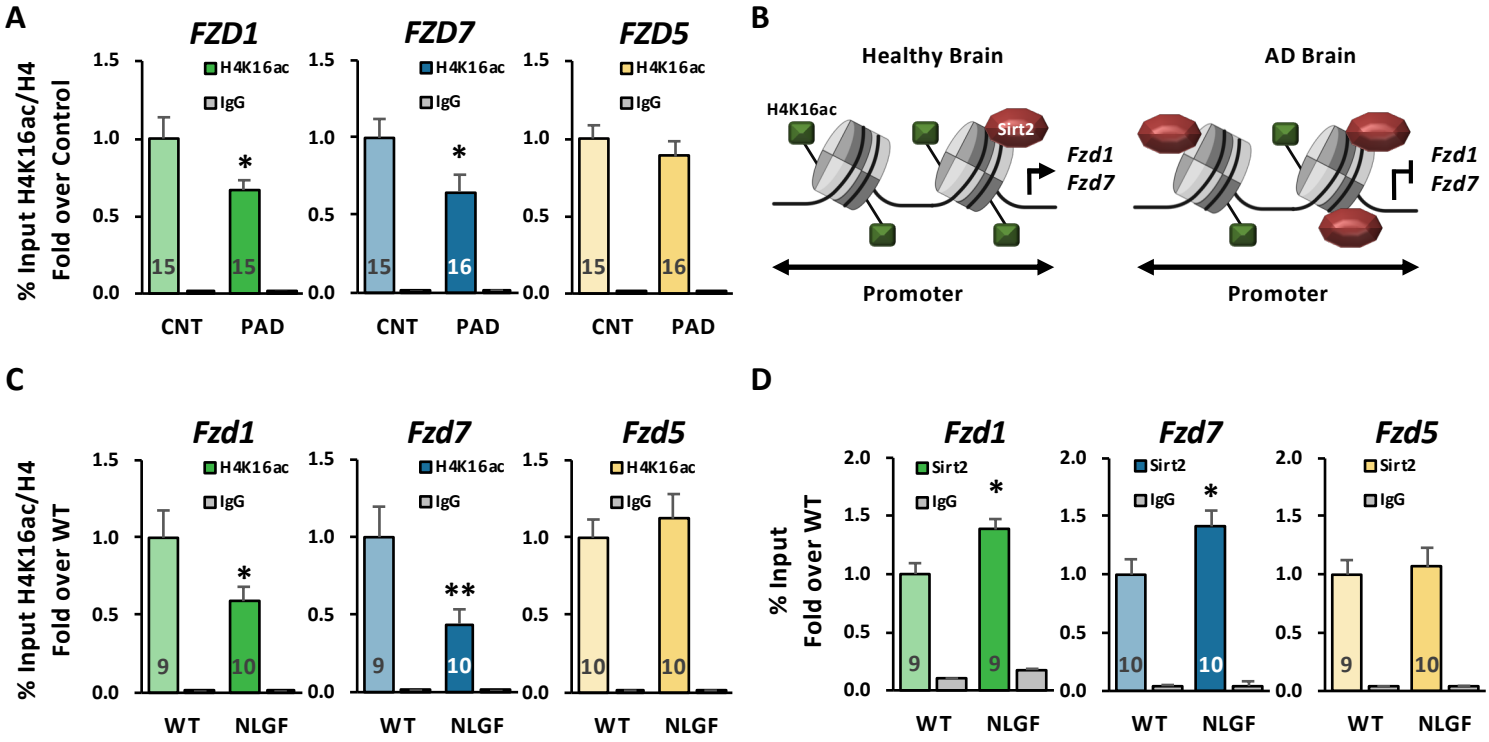
A
FZD1
FZD7
FZD5
H4K16ac
IgG
% Input H4K16ac/H4
Fold over Control
1.5
1.0
0.5
0.0
15
15
15
16
15
16
*
*
CNT
PAD
B
Healthy Brain
AD Brain
H4K16ac
Sirt2
Fzd1
Fzd7
Promoter
C
Fzd1
Fzd7
Fzd5
% Input H4K16ac/H4
Fold over WT
9
10
9
10
10
10
**
WT
NLGF
D
Sirt2
% Input
Fold over WT
2.0
9
9
10
10
9
10

Figure2

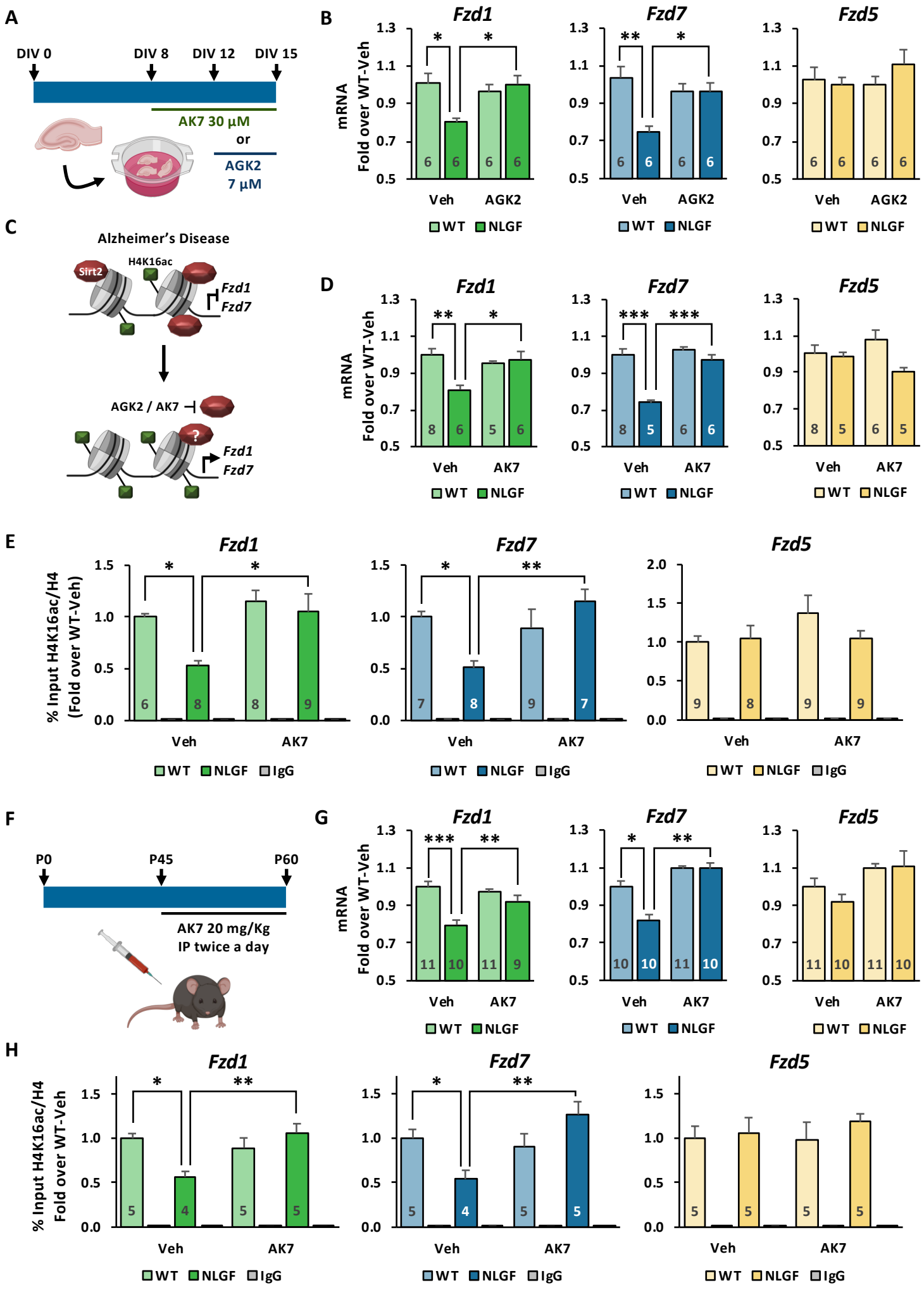
A
DIV 0
DIV 8
DIV 12
DIV 15
AK7 30 µM
or
AGK2
7 µM
B
Fzd1
Fzd7
Fzd5
mRNA
Fold over WT-Veh
Veh
AGK2
WT
NLGF
C
Alzheimer's Disease
Sirt2
H4K16ac
Fzd1
Fzd7
AGK2 / AK7
?
D
AK7
E
% Input H4K16ac/H4
(Fold over WT-Veh)
IgG
F
P0
P45
P60
AK7 20 mg/Kg
IP twice a day
G
H
% Input H4K16ac/H4
Fold over WT-Veh

Figure3

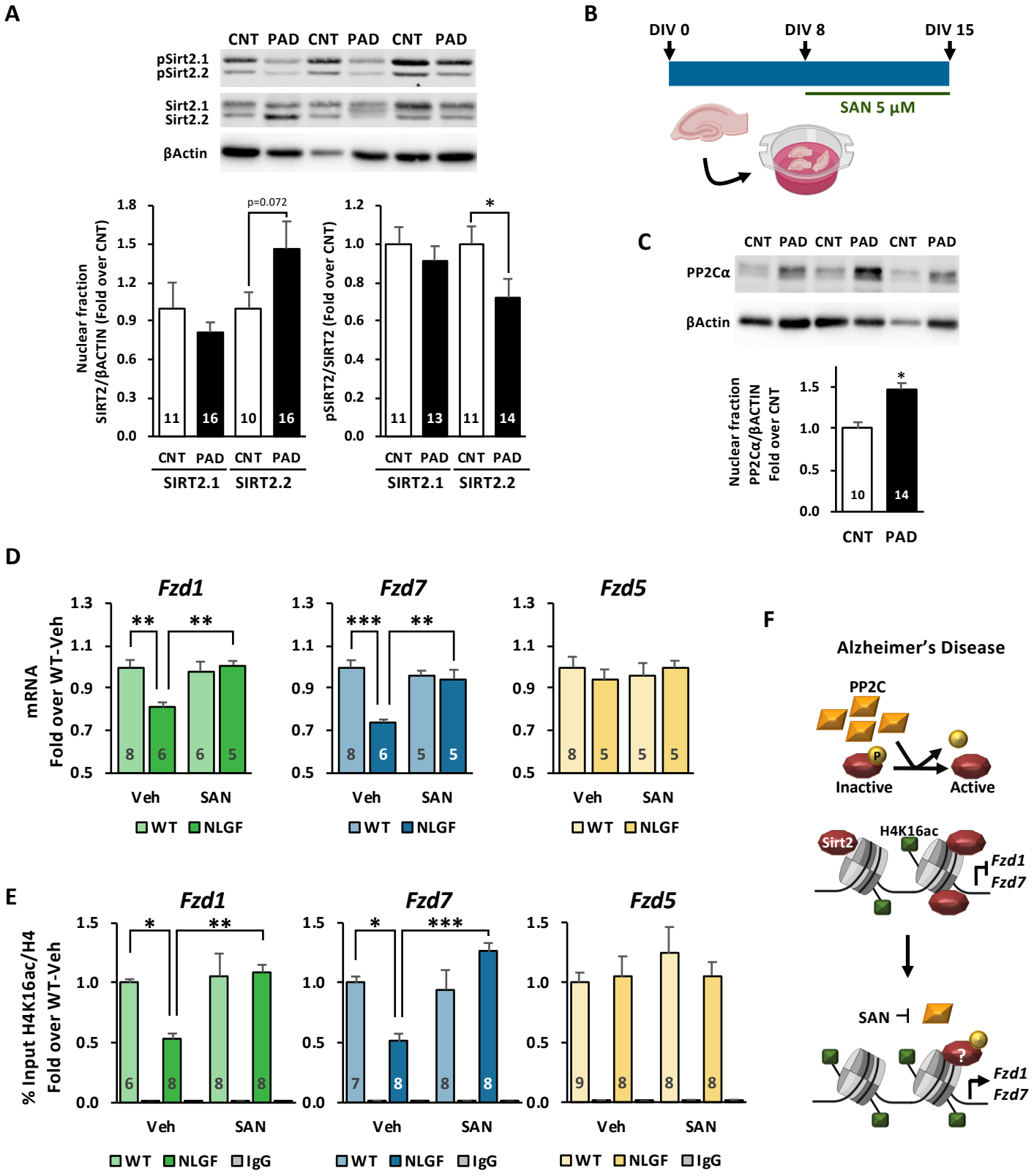
A
CNT PAD CNT PAD CNT PAD
pSirt2.1
pSirt2.2
Sirt2.1
Sirt2.2
βActin
Nuclear fraction SIRT2/βACTIN (Fold over CNT)
p=0.072
pSIRT2/SIRT2 (Fold over CNT)
CNT PAD CNT PAD
SIRT2.1 SIRT2.2
B
DIV 0
DIV 8
DIV 15
SAN 5 μM
C
PP2Cα
βActin
Nuclear fraction PP2Cα/βACTIN Fold over CNT
D
Fzd1
Fzd7
Fzd5
mRNA Fold over WT-Veh
Veh SAN
WT NLGF
E
% Input H4K16ac/H4 Fold over WT-Veh
IgG
F
Alzheimer's Disease
PP2C
Inactive
Active
Sirt2
H4K16ac
SAN

Figure 4

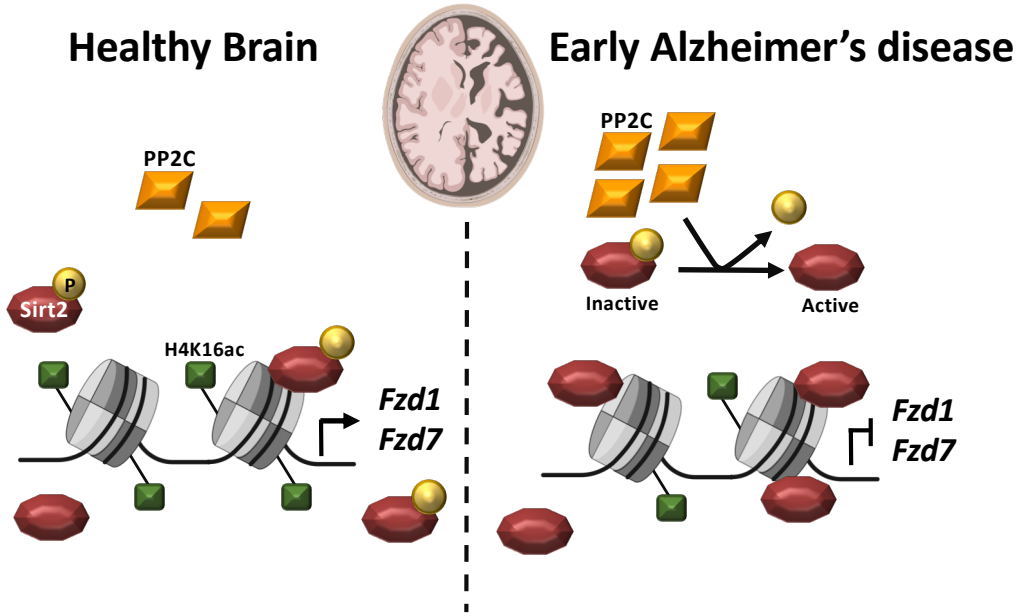
Healthy Brain
Early Alzheimer's disease
PP2C
Sirt2
P
H4K16ac
Fzd1
Fzd7
PP2C
Inactive
Active
Fzd1
Fzd7

Figure 5